Bifurcations of Relaxation Oscillations near Folded Saddles[*]

John Guckenheimer[†]   Kathleen Hoffman[‡]   Warren Weckesser[§]

December 7, 2004

Abstract

Relaxation oscillations are periodic orbits of multiple time scale dynamical systems that contain both slow and fast segments. The slow-fast decomposition of these orbits is defined in the singular limit. Geometric methods in singular perturbation theory classify degeneracies of these decompositions that occur in generic one parameter families of relaxation oscillations. This paper investigates the bifurcations that are associated with one type of degeneracy that occurs in systems with two slow variables, namely orbits that become homoclinic to a folded saddle.

1 Introduction

This paper investigates three dimensional dynamical systems of the form

$$\begin{aligned}
\varepsilon \dot{x} &= f(x, y, z) \\
\dot{y} &= g(x, y, z) \\
\dot{z} &= h(x, y, z)
\end{aligned} \tag{1}$$

These systems are known as *singularly perturbed* or *slow-fast vector fields*. The systems have two time scales with ε the ratio of time scales. We call x the *fast variable* and y, z the *slow variables*. Rescaling time by setting $\tau = \varepsilon t$ in equation (1) gives the *layer* equations

$$\begin{aligned}
x' &= f(x, y, z) \\
y' &= \varepsilon g(x, y, z) \\
z' &= \varepsilon h(x, y, z)
\end{aligned} \tag{2}$$

[†]Mathematics Department, Cornell University, Ithaca, NY 14853

[‡]Department of Mathematics and Statistics, University of Maryland, Baltimore County, Baltimore, MD 21250

[§]Mathematics Department, Colgate University, Hamilton, NY 13346

We call the equation $x' = f(x, y, z)$ the *fast subsystem*. In the singular limit $\varepsilon \to 0$, (1) is the differential algebraic equation

$$
\begin{aligned}
0 &= f(x, y, z) \\
\dot{y} &= g(x, y, z) \\
\dot{z} &= h(x, y, z)
\end{aligned}
\tag{3}
$$

The algebraic equation $f(x, y, z) = 0$ defines a surface called the critical manifold $\mathcal{C}$. On the critical manifold, the differential-algebraic equation reduces to an ordinary differential equation that defines the *slow flow* after a rescaling introduced below.

Neither (3) nor (2) captures the limits of solutions of (1) for $\varepsilon > 0$. The trajectories instead converge to objects that are called *candidates*[3, p. 68]. Candidates are concatenations of trajectory segments of (3) on the critical manifold and trajectories of the layer equations. The partition of a candidate into these trajectory segments is its *slow-fast decomposition*. *Relaxation oscillations* are ε-dependent families of periodic orbits of (1) that, as $\varepsilon \to 0$, converge to candidates with both slow and fast segments. We characterize below what we mean by *non-degenerate* slow-fast decompositions of candidates in terms of transversality conditions that relate the slow flow to the geometry of the critical manifolds.

Regular points of the critical manifold $\mathcal{C}$ are defined as those that satisfy the inequality $f_x \neq 0$. The stability of the regular points with respect to the fast subsystems is determined by the sign of f_x, with stability if $f_x < 0$ and instability if $f_x > 0$. The *fold curve S* of the critical manifold $\mathcal{C}$ is the set of points (x, y, z) that satisfy $f_x(x, y, z) = 0$. The fold curve can also be described as the set of singularities of the projection of $\mathcal{C}$ onto the plane of slow variables. The direction field of the slow flow can be extended to include the fold points by rescaling the slow flow. We differentiate $f(x, y, z) = 0$ with respect to time, solve for $\dot{x}$ and substitute values for $\dot{y}$ and $\dot{z}$ to obtain.

$$
\dot{x} = -\frac{f_z h + f_y g}{f_x}.
$$

Rescaling time by the function $-f(x)$ yields the *slow flow* equations

$$
\begin{aligned}
\dot{x} &= f_z h + f_y g \\
\dot{y} &= -f_x g \\
\dot{z} &= -f_x h,
\end{aligned}
\tag{4}
$$

which is readily seen to be tangent to the critical manifold. Note that the rescaling reverses the orientation of trajectories on the unstable sheets of the critical manifold since $f_x > 0$ there. However, candidates are defined to retain their original orientation for (3) before the time rescaling by $-f_x$.

Equilibrium points of the slow flow on the fold curve of the critical manifold occur when $f_z h + f_y g = 0$. These points are referred to as *folded singularities*. They can be classified

2

as equilibrium points of the two dimensional flow (4) restricted to the critical manifold $\mathcal{C}$. For example, the linearization of a folded saddle has one positive real eigenvalue and one negative real eigenvalue. The slow flow is said to satisfy the *normal switching conditions* at points where $f_z h + f_y g \neq 0$. Geometrically, the normal switching conditions imply that trajectories of the slow flow are orthogonal to the fold curve [13, 11].

We impose three conditions on the system (1) throughout the remainder of this paper:

- The critical manifold is a manifold; i.e., 0 is a regular value of f.

- The fold curve, defined by $f = f_x = 0$ is a smooth curve, and $f_{xx} = 0$ only at isolated points along this curve.

- The folded singularities are hyperbolic.

These conditions are generic within the class of smooth slow-fast systems with two slow variables and one slow variable [1], and we assume that they are satisfied throughout the remainder of the paper.

Let p be a point of the fold curve where $f_{xx} \neq 0$ and the normal switching conditions are satisfied. Then p is a semi-stable equilibrium point of its fast subsystems; i.e., p is the α-limit set of one trajectory and the ω-limit set of another trajectory for the one dimensional fast subsystem. If a trajectory of the slow flow arrives at p, then another trajectory of (3) arrives at p from the opposite side of the fold curve on the critical manifold $\mathcal{C}$. Therefore, there is only one candidate that continues from p, namely the fast trajectory whose α-limit set is p. If this trajectory is bounded, then its ω-limit set is another point q of $\mathcal{C}$. We define $J(p) = q$ on the set where $f_{xx} \neq 0$ and the normal switching conditions are satisfied, and call J the *jump map* of the fold curve. The jump map is defined on an open set of the fold curve, and it is smooth at p if $J(p)$ is a regular point of $\mathcal{C}$. Within this framework, we say that the slow-fast decomposition of a relaxation oscillation is *nondegenerate* if it satisfies the following two conditions:

- Transitions from slow to fast segments occur at points p where $f_{xx} \neq 0$ and the normal switching conditions are satisfied. Thus, the jump map $J(p)$ is defined.

- $J(p)$ is a regular point of $\mathcal{C}$ and the image of J is transverse to the slow flow at p.

We remark that the set of slow-fast systems with relaxation oscillations satisfying these conditions is open, but it is not dense in the space of slow-fast systems. In particular, there are open sets of systems that have relaxation oscillations containing folded-nodes[3, 8, 14]. We do not consider such relaxation oscillations in this paper.

Our primary interest is in understanding bifurcations of one parameter families of relaxation oscillations. We assume that the system (1) depends upon an *extrinsic* parameter λ as well as its *intrinsic* parameter ε. If $\gamma_{\lambda,\varepsilon}$ is a family of relaxation oscillations, we study bifurcations of γ with varying λ while ε is small. In the singular limit, degeneracies of the slow-fast decomposition can give rise to bifurcations. There are several types of degeneracies

3

that occur within generic one parameter families []. A separate analysis of the bifurcations associated to each type of degeneracy is needed. We consider here bifurcations associated to the degeneracy in which a candidate contains a folded saddle. Examples are the homoclinic bifurcations in the reduced system of the forced van der Pol equation [10, 4]. These are discussed in Section §4 below.

2   Folded saddles

Folded saddles in three dimensional slow-fast systems have been analyzed by Benoit [2] with techniques from nonstandard analysis and by Szmolyan and Wechselberger from a geometric perspectiv[qe [13]. See also Arnold et al. [1] and Guckenheimer [7]. The local analysis of folded saddles describes the geometry of the flow of the "full" three dimensional system near the folded saddle.

The flow around the folded saddle can be approximated by a simpler system. Through a combination of linear and near-identity coordinate transformations, system (1) can be transformed into

$$
\begin{aligned}
\varepsilon \dot{x} &= y - x^2 + O(\varepsilon x, \varepsilon y, \varepsilon z, xy^2, x^3, xyz) \\
\dot{y} &= az + bx + O(y, \varepsilon, z^2, xz, x^2) \\
\dot{z} &= 1 + O(x, y, z, \varepsilon),
\end{aligned}
\tag{5}
$$

in the neighborhood of a folded saddle [1]. By using the rescaling $x \to \varepsilon^{1/2} x$, $y \to \varepsilon y$, $z \to \varepsilon^{1/2} z$, and $t \to \varepsilon^{1/2} t$, and dropping the higher order terms, we obtain the system of first approximation:

$$
\begin{aligned}
\dot{x} &= y - x^2 \\
\dot{y} &= az + bx \\
\dot{z} &= 1.
\end{aligned}
\tag{6}
$$

System (6) provides a local model for the folded saddle that we use in a manner analogous to the use of the linearization of an equilibrium point as a local model for the flow near a hyperbolic equilibrium. Thus, the dynamics of (6) are a central component of the analysis of bifurcation at folded saddles. We shall also use the system

$$
\begin{aligned}
\varepsilon \dot{x} &= y - x^2 \\
\dot{y} &= az + bx \\
\dot{z} &= 1.
\end{aligned}
\tag{7}
$$

that is an ε dependent scaling of (6).

The coefficients a and b in (6) are functions of f, g, h that can be computed from its linearization at the folded saddle. If we rewrite (5) in terms of the variables x and z and

4

rescale time, as was done previously for (1) and linearize, we get

$$\dot{x} = bx + az,$$
$$\dot{z} = 2x \tag{8}$$

The eigenvalues of the linear system (8) depend on the parameters a and b. This system has a saddle at the origin if $a > 0$. The sign of b plays an important role in determining the bifurcations in the full system.

The critical manifold of systems (5) and (7) are close to the paraboloid $y = x^2$, and their fold curves are close to the z-axis. The theory of normal hyperbolicity implies that (7) has a unique invariant surface S_a that remains at a bounded distance from $y = x^2$, $x > 0$ as trajectories are followed backward in time and a unique invariant surface S_r that remains at a bounded distance from $y = x^2$, $x < 0$ as trajectories are followed forward in time. These surfaces are the stable and unstable sheets of the "true" slow manifold of (7), respectively.

The system (6) has two exact solutions

$$\begin{aligned} x(t) &= \alpha t \\ y(t) &= \alpha + \alpha^2 t^2 \\ z(t) &= t, \end{aligned}$$

where α is one of the roots of the equation

$$2\alpha^2 - b\alpha - a = 0. \tag{9}$$

The two exact solutions are the *maximal canard* and the *faux maximal canard* corresponding to the roots α_n and α_p, the positive and negative roots of (9), respectively. *Canards* are solutions that contain segments of positive length near S_r. Clearly, the maximal canard lies in the intersection of $S_a \cap S_r$. Using a variational argument, Benoit [3] proved that the intersection of $S_a \cap S_r$ is transverse.

For our purposes, we need additional information about the flow of system (1) near a folded saddle. In particular, we want to study the map that describes the passage of trajectories through a neighborhood of the folded saddle. Since we do not have analytic expressions for the flow of even (6), we resort to numerical computations of this system. We use the system (7) as a model, relying upon the theory of parameter dependent blowups [13], to compare the flows of (1) and (7).

The flow of (6) is transverse to sections with z constant, so we introduce cross-sections at $z = z_0 < 0$ and $z = z_1 > 0$ and integrate the system between these sections. We know that all the solutions starting in a neighborhood of the critical manifold for a value of $z_0 < 0$ with large magnitude are attracted to an exponentially small neighborhood of the slow manifold, so the image of the map along trajectories will have an image that is almost one dimensional. Figure 1 depicts this flow with $z_0 = -5$, $z_1 = 3$, $a = 3$ and $b = -1$, showing portions of trajectories that begin on the critical manifold at $z_0 = -5$ between the planes $z = -5$ and $z = 3$. Figure 2 shows projections of the flow of (6) onto the (x, z) plane.
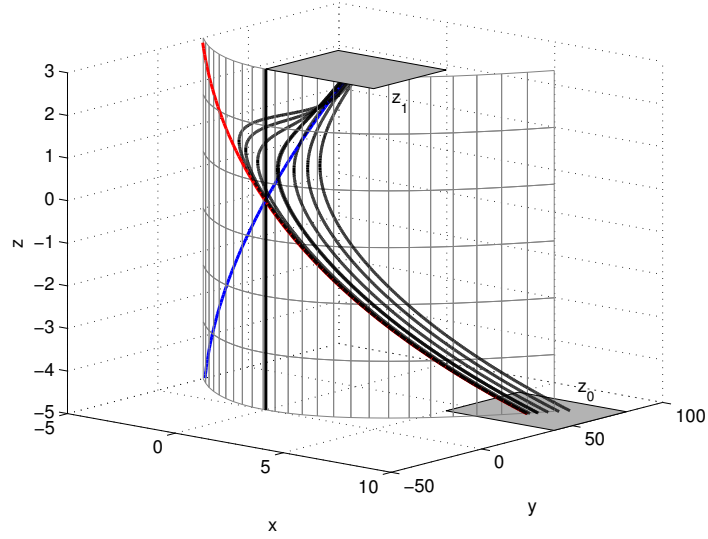
5

Figure 1: This figure illustrates solutions to (6). The red and blue curves are the maximal canard and faux maximal canard, respectively. The mesh represents the critical manifold of (1). The remaining curves show trajectories starting in $z = z_0$=-5 and ending in $z = z_1 = 3$.
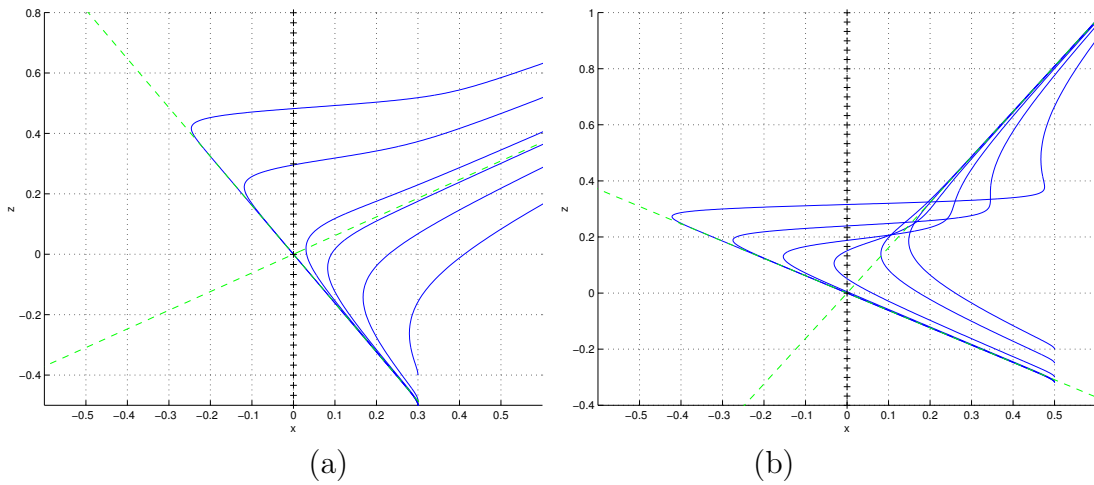

Figure 2: Flow of system (6) projected onto the (x, z) plane. The green dashed lines are the eigenspaces of the slow flow, and the solid blue lines are numerical solutions to system (6) (a) $a = 3$, $b = 1$, (b) $a = 3$, $b = -1$.

For system (7), we denote the map along trajectories between $z = z_0 < 0$ and $z = z_1 > 0$ by Ψ_ε and the corresponding map for (8) we call Ψ_0. We analyze Ψ_0 as an approximation to Ψ_ε as $\varepsilon \to 0$. The results depend crucially upon the sign of b. The eigenvalues of (8) are $\mu_\pm = \frac{1}{2}(b \pm \sqrt{(b^2 + a)})$ and the corresponding eigenvectors are $(\mu_\pm/2, 1)$. The right half plane $x > 0$ corresponds to the stable sheet S_a of the slow manifold. The stable manifold of the saddle point of Ψ_0 has a separatrix in the fourth quadrant. Trajectories below this separatrix flow to the fold curve along the z-axis, while trajectories above the separatrix remain in the half plane $x > 0$. Thus, the map Ψ_0 is defined above the separatrix and has a singularity of the form $(x - x_s)^\alpha$. Here $x_s = \mu_m z_0/2$ is the value of x at the intersection of the stable manifold of the saddle with the cross-section $z = z_0$ and $\alpha = -\mu_m/\mu_p$ is the magnitude of the ratio of the stable eigenvalue to the unstable eigenvalue. When $b > 0$, $\alpha < 1$ and the slope of Ψ_0 approaches ∞ as $x \to x_s^+$. When $b < 0$, $\alpha > 1$ and the slope of Ψ_0 approaches 0 as $x \to x_s^+$.

To represent canards in the slow flow (8), we follow the stable manifold of the saddle *through* the origin into the second quadrant. When the trajectory reaches its jump point, it jumps from the unstable sheet of the slow manifold to the stable sheet parallel to the x-axis; i.e., the point (x, z) jumps to $(-x, z)$. From $(-x, z)$ the trajectory resumes its motion under the slow flow. See Figure 3. We can regard the canards as appending a vertical segment to the graph of Ψ_0. In the case that $b > 0$, the slope of the stable manifold has smaller magnitude than the slope of unstable manifold, so the image of the jumps gives a curve that lies below the unstable manifold in the first quadrant. Consequently, the vertical segment we append to the graph of Ψ_0 extends *down* from $x_1 = \mu_+ z_1/2$, the value of x at the intersection of the unstable manifold with the section $z = z_1$. In the case that $b < 0$, the slope of the stable manifold has larger magnitude than the slope of unstable manifold, so the image of the jumps gives a curve that lies above the unstable manifold in the first quadrant. Consequently, the vertical segment we append to the graph of Ψ_0 extends *up* from $x_1 = \mu_+ z_1/2$, the value of x at the intersection of the unstable manifold with the section $z = z_1$. The extended graph has a local minimum at the stable manifold as depicted in the dashed curve of Figure 4.

The map Ψ plays a central role in our analysis of bifurcations of relaxation oscillations at folded saddles. In the case $b < 0$, we need to determine how the singular map Ψ_ε changes as $\varepsilon \to 0$. Lacking analytical solutions of system (7), we resort to numerical simulations. Figure 4 plots data about the map along trajectories for parameter values $a = 3$ and $b = -1$ and three different values of ε. With initial conditions starting on the critical manifold in the cross-section $z = -5$, we compute the value of x in the cross-section $z = 5$. The stable manifold of the folded saddle in the slow flow 8 intersects the initial cross-section at $x = 7.5$. It is apparent in these simulations that the map Ψ restricted to a curve of initial conditions lying on the critical manifold has non-zero second derivative in a neighborhood of its local minimum.
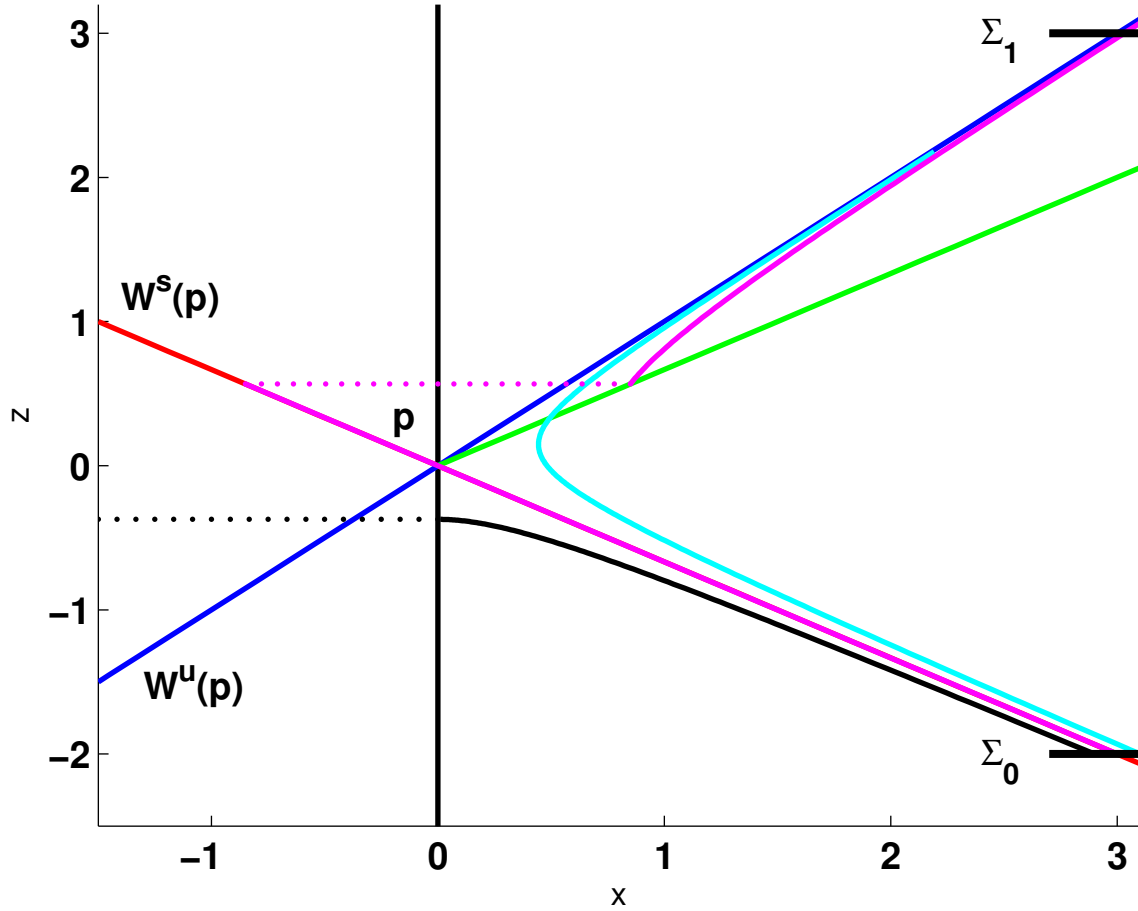
Figure 3: The representation of trajectories with canards in the slow flow (8). The stable manifold of the saddle point p is drawn red, the unstable manifold of p is drawn blue. The black trajectory reaches the fold curve and makes a jump (dotted). The light blue trajectory lies on the turn side of the stable manifold. The magenta trajectory proceeds through p along the stbale manifold, jumps back to the stable sheet of the critical manifold (dotted) and then continues on the stable sheet. The green ray is the locus of end points for jumps back from canards on the unstable sheet of the critical manifold to the stable sheet.
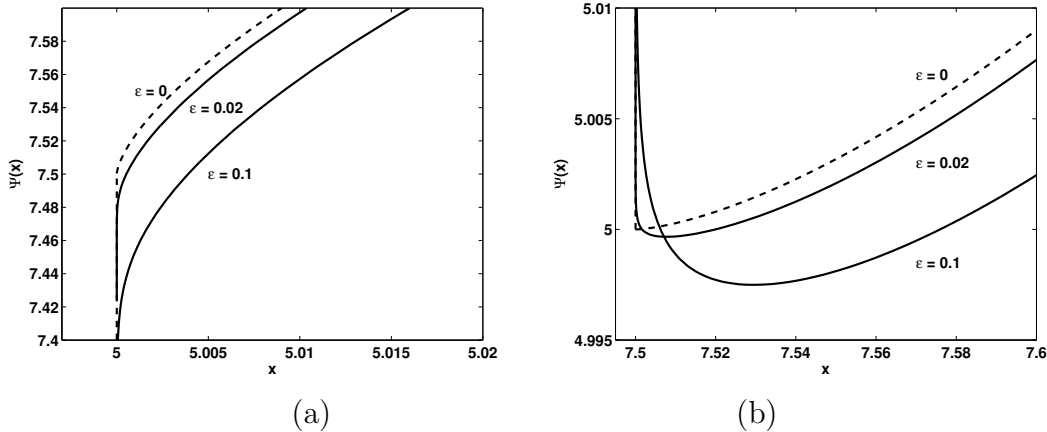
Figure 4: Plots of the singular input-output map for the cases $b > 0$ and $b < 0$.

3 Bifurcations of Relaxation Oscillations near Folded Saddles

This section states the main results in this paper. We combine local models for flow near a folded saddle with "global returns" to develop a picture of how relaxation oscillations bifurcate when they approach a folded saddle. This type of analysis was pioneered by Silnikov in his analysis of (single time scale) systems with homoclinic orbits to focal saddles [12]. We begin by introducing terminology that distinguishes different types of families of relaxation oscillations that approach a folded-saddle.

Consider the singular limit (3) of system (1). Assume that there is a folded saddle p with stable manifold $W^s(p)$ and unstable manifold $W^u(p)$ for the slow flow. Let Σ be a cross section at q to $W^s(p)$ on the stable sheet of the critical manifold. See Figure 3. Points that start on Σ to one side of q flow directly to the fold curve and then jump, while points on the opposite side of q follow $W^u(p)$ away from p. We call these the *jump* and *turn* sides of $W^s(p)$, respectively. Relaxation oscillations of (1) that come close to p will have fixed points for the return map θ of Σ. The map θ has a discontinuity at q due to the different directions taken by trajectories on the jump and turn sides of $W^s(p)$. We have $\theta'(x) \to \infty$ as $x \to q$ on the jump side of q [10], while the limit of $\theta'(x)$ as $x \to q$ on the turn side of q depends on the trace of the Jacobian of the (rescaled) slow flow at p. In the case of positive trace, the limit is ∞, while in the case of negative trace, the limit is 0.

Consider the system (1) with an active parameter λ that we vary in addition to ε. We denote these systems by $X_{\lambda,\varepsilon}$ and assume that there is a family of relaxation oscillations $\gamma_{\lambda,\varepsilon}$ that contains the folded saddle p in its closure. We want to determine what types bifurcations to expect in generic families. Typically, such families will have a portion that consists of nondegenerate relaxation oscillations and a portion consisting of relaxation oscillations that contain canards. In the singular limit, the orbits containing canards have the same parameter

λ_c. The candidates with canards contain varying portions of the unstable manifold of p on the unstable sheet of the critical manifold. It might happen that there are bifurcations that occur within the interior of the family of orbits with canard segments, but that is not our concern here. Here we focus upon bifurcations of periodic orbits in the family that have limits at the transition between the nondegenerate relaxation oscillations and those containing canards.

Families on the jump side of $W^s(p)$ will not have bifurcations at the transition between nondegenerate relaxation oscillations and relaxation oscillations containing canards. The return map θ on the jump side of $W^s(p)$ has vertical extensions that prolong a steep portion of the graph of θ without creating turning points. As λ varies, extended graphs with fixed points on the vertical segments correspond to relaxation oscillations with canards. Similarly, if the Jacobian at p has positive trace, families on the turn side of $W^s(p)$ will not have bifurcations at the transition between nondegenerate relaxation oscillations and relaxation oscillations containing canards. In the last section, we have shown that the vertical extensions of θ on the turn side also prolong a steep portion of the graph of θ without creating turning points.

In the remaining case of families of relaxation oscillations on the turn side of $W^s(p)$ and negative trace for the Jacobian at p, θ has a local extremum and there will be bifurcations.

Conjecture 1 *Let $\gamma_{\lambda,\varepsilon}$ be a generic family of relaxation oscillations for the slow-fast vector field $X_{\lambda,\varepsilon}$ with two slow and one fast variable. Assume that*

- *The slow-fast decompositions of $\gamma_{\lambda,0}$ are nondegenerate for $\lambda < \lambda_0$.*

- *As $\lambda \to \lambda_0$, the candidates $\gamma_{\lambda,0}$ approach a candidate γ_0 that is a closed curve containing segments of the stable manifold $W^s(p)$ and unstable manifold $W^u(p)$ of a folded saddle p on the stable sheet of the critical manifold.*

- *The trace of the Jacobian at the folded saddle p is negative.*

- *The intersections of $W^s(p)$ and candidates that begin on $W^u(p)$ with the cross-section Σ on the critical manifold cross transversally at $\lambda = \lambda_0$ as λ varies.*

Then $\gamma_{\lambda,\varepsilon}$ undergoes either saddle-node bifurcation of periodic orbits or period doubling bifurcation as λ varies near λ_0, $\varepsilon > 0$ is small. The bifurcating periodic orbits tend to γ_0 as $\varepsilon \to 0$. Which case occurs depends upon the sign of the return map θ for the nondegenerate relaxation oscillations. If the orbits on the turn side of $W^s(p)$ return with positive slope, then the families have a period doubling bifurcation. If the orbits on the turn side of $W^s(p)$ return with negative slope, then the families have a saddle-node of periodic orbits bifurcation.

This conjecture is based upon the numerical simulations described in the previous section. We interpret those results as demonstrating that the return maps for the family can be rescaled in the vicinity of the stable manifold of the folded saddle so that they converge to "blown up" one dimensional return maps for the singular limit that have nondegenerate

critical points. With our assumptions and conjectures, the blown up return maps in the singular limit are generic families of one dimensional maps. While this argument can be amplified beyond these remarks, a proof of these conjectures depends upon verification of the numerical results we have obtained for flow past the folded saddle.

4   Horseshoes

The period doubling bifurcations described in the previous section are at the beginning of cascades that produce horseshoes. We describe how this happens in this section. Of the cases considered in the previous section, the only one that exhibits horseshoes in the transition region between regular orbits and canards is the one with negative trace Jacobian and a return map for which the slope at the turn side trajectories is positive.

We regard the return maps θ for the full system as perturbations of one dimensional maps. The fast contraction along the stable sheets of the slow manifold will be stronger than any expansion that occurs during the slow flow along these sheets, during jumps or in the transition region where canards begin to form. The Jacobian of the return maps for the transition regions will be exponentially small. More specifically, there is a constant $\bar{c} > 0$ such that $\det(D\theta) < \exp(-\bar{c}/\varepsilon)$. We assume that outside of regions where θ has a fold that there is a strong contracting foliation, and that projection along this foliation produces a one dimensional map $\bar{\theta}$ whose dynamical properties determine those of θ. Now, θ and $\bar{\theta}$ are compositions of transition maps past the folded saddle with a smooth diffeomorphism. The expansion and folding of $\bar{\theta}$ will be dominated by the flow past the folded saddle, and we model this with the maps Ψ_ε.

Our goal is to identify parameters for which the maps θ have chaotic invariant sets close to the stable manifold of the folded saddle. For this purpose, we apply the extensive theory of one dimensional maps [5] to $\bar{\theta}$. We seek maps $\bar{\theta}$ that have expanding invariant sets that are conjugate to subshifts of finite type. The simplest siutation is that there would be two disjoint subintervals A, B with $A \cup B \subset \bar{\theta}(A)$ and $A \cup B \subset \bar{\theta}(B)$, but this will not hold in the transition region that we study because $\bar{\theta}$ has only one fixed point in this region. Instead, we look for disjoint subintervals A, B with $B \subset \bar{\theta}(A)$ and $A \cup B \subset \bar{\theta}(B)$. This weaker requirement guarantees that there will be a subshift with transition map

$$\begin{pmatrix} 1 & 1 \\ 1 & 0 \end{pmatrix} \tag{10}$$

If z_c denotes the critical point of $\bar{\theta}$, the existence of such intervals, depends upon the first three iterates of z_c. These should be ordered so that $\bar{\theta}(z_c) < z_c < \bar{\theta}^3(z_c) < \bar{\theta}^2(z_c)$. Then the intervals $A = [\bar{\theta}(z_c), z_c]$ and $B = [z_c, < \bar{\theta}^2(z_c)]$ have the desired images.

Let z be coordinate along a curve I on the slow manifold of (1) that cuts the stable manifold of the folded saddle p transversally. There are three segments for I and its image that we consider:

Figure 5: The graph of the return map θ for a parameter value at which there will be a chaotic invariant set.

- the regular trajectories on the turn side of $W^s(p)$ where the slope of θ is z^α with $-\alpha$ the ratio of the eigenvalues at the folded saddle.

- a neighborhood of radius $O(\varepsilon^{1/2})$ where numerical simulations of the system (7) indicate that $\bar\theta$ has a critical point z_c with nonzero second derivative.

- a canard region where the slope of the return map is exponentially large; i.e of magnitude $O(\varepsilon(c/\varepsilon))$

See Figure 5. If $\partial_\lambda \bar\theta + \partial_{\lambda z} \bar\theta / \partial_{zz} \bar\theta$ is nonzero, then the distance $z_c - \bar\theta(z_c)$ depends in a non-singular way upon λ. We can achieve values of $\bar\theta^2(z_c) - z_c$ that are $O(1)$ for values of $z_c - \bar\theta(z_c)$ that are $O(\varepsilon)^{1/2}$. In this case, $\bar\theta^{-1}(z_c) - z_c$ is $O(\varepsilon)^{1/4}$, so we will have $z_c < \bar\theta^3(z_c) < \bar\theta^2(z_c)$ as desired.

We would also like to verify that the chaotic invariant sets we identify are hyperbolic. To do so, we examine $\bar\theta'$ on intervals contained in $[\bar\theta(z_c), z_c]$ and $(\bar\theta^2)'$ on intervals contained in $[z_c, \bar\theta^2(z_c)]$. There is $z_3 \in [\bar\theta(z_c), z_c]$ with $\bar\theta(z_3) \in [\bar\theta(z_c), z_c]$, $\bar\theta^2(z_3) \in [z_c, \bar\theta^2(z_c)]$ and $\bar\theta^3(z_3) = z_3$. We can take $A = [\bar\theta(z_3), z_3]$ and $B = [\bar\theta^{-1}(z_3), \bar\theta^2(z_3)]$. As $z_c - \bar\theta(z_c)$ increases, the slope on A becomes exponentially large, while the slope on B is at least $O(\varepsilon^{1/2})$. These estimates suggest that $\bar\theta$ will be expanding on the invariant set contained in $A \cup B$. Therefore, we conjecture that the period doubling bifurcations described in the preceding section will be followed by cascades producing chaotic invariant sets when ε is sufficiently small.

5   The Forced van der Pol System

In this section, we apply the theory described in §3 to the forced van der Pol equation, written as as the following vector field on $\mathbb{R}^2 \times S^1$:

$$
\begin{aligned}
\varepsilon \dot{x} &= y + x - \frac{x^3}{3} \\
\dot{y} &= -x + a\sin(2\pi\theta) \\
\dot{\theta} &= \omega.
\end{aligned}
\tag{11}
$$

We regard $S^1 = \mathbb{R}/\mathbb{Z}$ and use coordinates $[0, 1]$ for S^1, understanding that the endpoints are identified. We have studied the dynamics of the forced van der Pol equation previously [10, 4], including computations of bifurcations in it reduced system that produce homoclinic orbits to a folded saddle.

The rescaled slow flow of equation (11) is the vector field

$$
\begin{aligned}
\theta' &= \omega(x^2 - 1) \\
x' &= -x + a\sin(2\pi\theta).
\end{aligned}
\tag{12}
$$

on $S^1 \times \mathbb{R}$. The vector field (12) is obtained from the forced van der Pol equation (11) by differentiating the algebraic equation $y = x^3/3 - x$ of the critical manifold to obtain $\dot{y} = (x^2 - 1)\dot{x}$, substituting the result into the van der Pol equation (11) and rescaling time by $(x^2 - 1)$. Note that with this change of coordinates, time has been reversed for $|x| < 1$. The equilibrium points of the slow flow lie at the points $(\theta, x) = (\pm \sin^{-1}(1/a)/2\pi, \pm 1)$. Here $\sin^{-1}$ is regarded to be a double valued "function" on $(-1, 1)$. If $a > 1$, there are four equilibrium points, two of which are saddles. In this system, the Jacobian of the saddles of the slow flow always have negative trace.

The slow flow of the forced van der Pol equation (12) contains a symmetry, namely $T(\theta, x) = (\theta + \frac{1}{2}, -x)$, that can be exploited when defining the global return map. We define a half return map $H = (TJ_+P_+)$, where T is the symmetry operator, $P_+ : S_{-2} \to S_1$ is a map that follows the flow along the critical manifold from the circle $x = -2$ to the circle $x = 1$, and $J_+ : S_1 \to S_{-2}$ approximates the fast subsystem, by imposing a jump from the fold on the critical manifold from $x = 1$ to $x = -2$. It can be shown [9] that the square of this half return map H defines a global return map for the system (12). This map and its bifurcations were carefully studied in [9].

Homoclinic bifurcations for the slow flow of the forced van der Pol equation can be described analytically by defining equations for its half return map. In our earlier work we denoted homoclinic bifurcations on the jump side of the folded saddle as 'left' homoclinic bifurcations and homoclinic bifurcations on the turn side of the folded saddle as 'right' homoclinic bifurcations. The turn side homoclinic bifurcations were further delineated by the number of times the stable manifold of the saddle intersects $x = 2$ along the homoclinic orbit. Since we trace of the saddle Jacobian is negative, the slope of the turn side segments of the half return map approach 0 at their endpoints. Figure 6 shows graphs of the half return maps for jump side and turn side homoclinic bifurcations in parameter regimes where H has a single discontinuity. The slope at turn side homoclinic bifurcation is positive. The slope at turn side homoclinic bifurcations is negative where the homoclinic orbit corresponds to the second intersection of the stable manifold of the saddle with the line $x = 2$. This happens for larger values of a in (12). The canard extensions of the half return map H extend vertically upward, so the turn side homoclinic bifurcations with positive slope give rise to period doubling bifurcations while the turn side homoclinic bifurcations with negative slope give rise to saddle-node bifurcations of periodic orbits in the full system. Note that period 2 orbits of H correspond to either a single symmetric periodic orbit of the continuous time flow with doubled period, or to a pitchfork bifurcation that produces a pair of asymmetric periodic orbits whose period has not doubled. In the example that we study, period doubling of H is period doubling: it produces a single symmetric periodic orbit of the continuous time flow of period 6.

Figures 7 and 7 show numerical calculations of bifurcation diagrams for the period doubling and saddle-node cases of period 3 orbits of the forced van der Pol system (11), computed with the program AUTO [6]. In both sets of calculations, $\varepsilon = 0.002$, a is fixed and ω is the active bifurcation parameter. The period doubling calculations use $a = 1.8$ while the saddle-
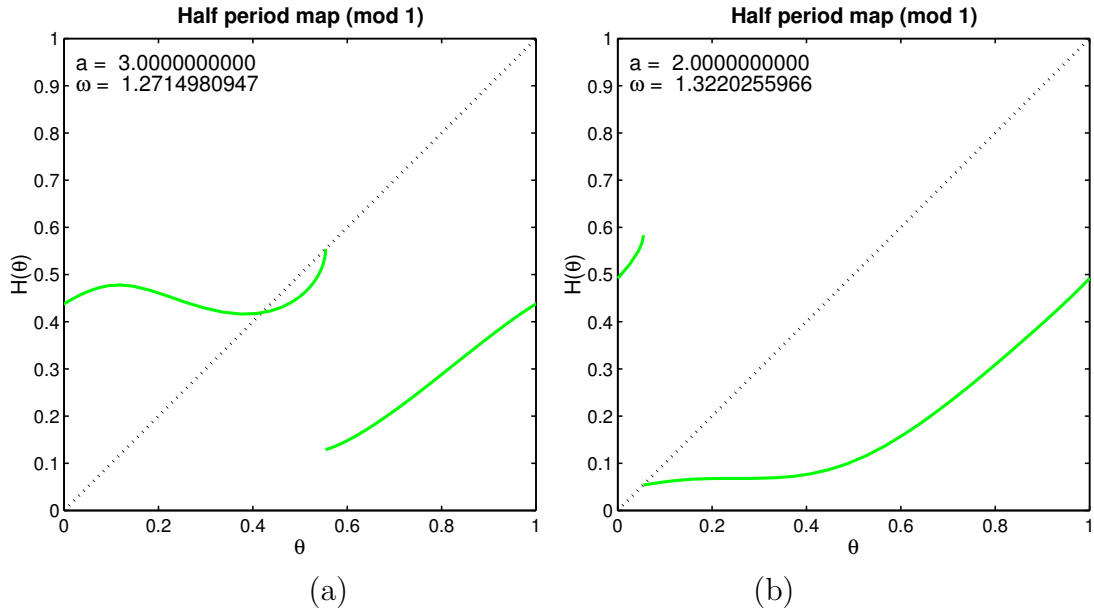
13

Figure 6: Figure (a) is a graph of the half return map for the forced van der Pol equation with a jump side homoclinic bifurcation and an infinite slope. Figure (b) is a graph of the half return map with parameters for which a turn side homoclinic bifurcation occurs with zero slope. Note the canard extensions are not shown in this figure.

node calculations use $a = 3.5$. The right hand panels show expanded views of neighborhoods of the bifurcations in the transition zones. The branch of period doubled, period 6 orbits bifurcates from the branch of period 3 orbits at the transition between period orbits with and without canards. The canards that form here are "jump back" canards that lie on the turn side of the stable manifold of the folded saddle. As predicted, when $a = 3.5$, there is a saddle-node bifurcation of periodic orbits that occurs at the transition between orbits with no canards and orbits with jump back canards. For both families of periodic orbits, there is a saddle-node bifurcation of periodic orbits that occurs in a region without canards. The branches of unstable orbits that form at these saddle-node bifurcations continue smoothly to periodic orbits with jump away canards. Note that there are additional bifurcations that occur along the family of period doubled orbits "deep" in the region where there are canards and our theory makes no predictions. These computations provide evidence for the validity of our conjectures.
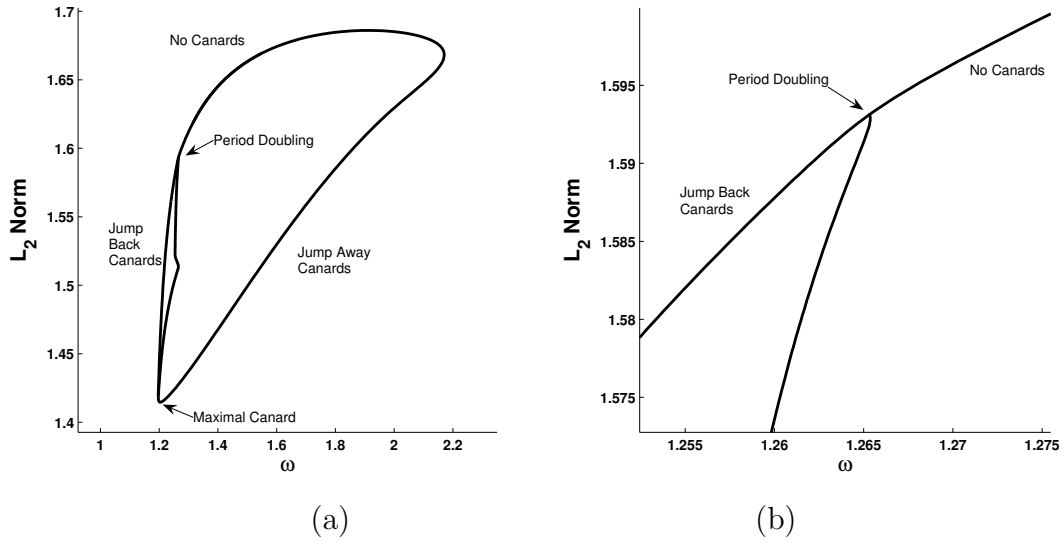
14

Figure 7: Bifurcations of period 3 orbits in the forced van der Pol system with $a = 1.8$, $\varepsilon = 0.002$ and varying ω. There is a period doubling bifurcation that occurs in the transition between orbits without canards and orbits with jump back canards. Panel (b) shows detail of this region.
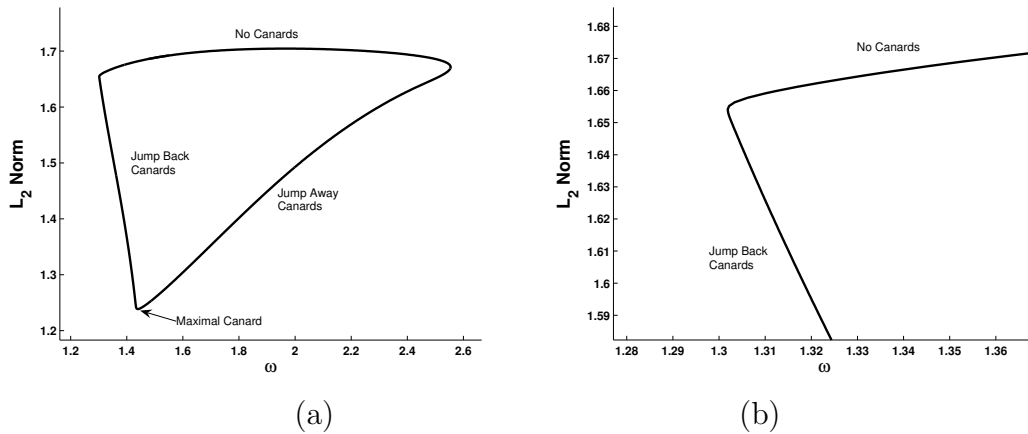

Figure 8: Bifurcations of period 3 orbits in the forced van der Pol system with $a = 3.5$, $\varepsilon = 0.002$ and varying ω. There is a saddle-node of periodic orbits bifurcation that occurs at the left hand turning point. The transition between orbits without canards and orbits with jump back canards occurs here. Panel (b) shows detail of this region.

References

[1] Arnold, V. I., Afrajmovich, V. S. Il'yashenko, Yu. S. and Shil'nikov, L.P. *Dynamical Systems V.* Encyclopaedia of Mathematical Sciences. Springer-Verlag, 1994.

[2] Benoît, É. Systmes lents-rapides dans R^3 et leurs canards. Third Schnepfenried geometry conference, Vol. 2 (Schnepfenried, 1982), 159–191, Astrisque, 109-110, Soc. Math. France, Paris, 1983.

[3] Benoît, É. Canards et enlacements *Publ. Math. IHES Publ. Math.* **72**(1990) 63–91

[4] K. Bold, C. Edwards, J. Guckenheimer, K. Hoffman, R. Oliva, W. Weckesser The forced van der Pol Equation II: Canards in the Reduced System, SIAM J. App. Dyn. Sys, **2**(4), p. 570-608, 2003.

[5] de Melo, W. and van Strien, S. One-dimensional dynamics. Ergebnisse der Mathematik und ihrer Grenzgebiete (3) [Results in Mathematics and Related Areas (3)], 25. Springer-Verlag, Berlin, 1993.

[6] E. Doedel, R. Paffenroth, A. R. Champneys, T. F. Fairgrieve, Y. A. Kuznetsov, B. Sandstede, and X. Wang. *AUTO 2000: Continuation and Bifurcation Software for Ordinary Differential Equations (with HomCont).* 2001.

[7] Guckenheimer, J. Bifurcation and degenerate decomposition in multiple time scale dynamical systems, in Nonlinear Dynamics and Chaos: where do we go from here?' edited by John Hogan, Alan Champneys, Bernd Krauskopf, Mario di Bernardo, Eddie Wilson, Hinke Osinga, and Martin Homer Institut of Physics Publishing, Bristol, pp. 1-21, 2002.

[8] Guckenheimer, J. Haiduc, R Canards at folded nodes accepted for publication at Moscow Mathematical Journal

[9] Guckenheimer,J K. Hoffman, and W. Weckesser, Global Bifurcations of Periodic Orbits in the Forced Van der Pol Equation in *Global Analysis of Dynamical Systems*, eds H.W. Broer, B. Krauskopf and G. Vegter, Institute of Physics Publishing, Dirac House, 2001

[10] Guckenheimer, J. Hoffman, K. and Weckesser, W. The Forced van der Pol Equation I: The Slow Flow and its Bifurcations, SIAM J. App. Dyn. Sys, **2**(1), p.1-35, 2003.

[11] Mischenko, E. Kolesov, Yu. Kolesov, A. and Rozov, N. *Asymptotic methods in singularly perturbed systems* (Translated from the Russian by Irene Aleksanova. New York: Consultants Bureau), 1994.

[12] Silnikov, L.P. A contribution to the problem of the structure of an extended neighborhood of a rough equilibrium point of saddle-focus type. Math. USSR Sb., **10**(1), 91-102, 1970.

[13] Szmolyan, P. and Wechselberger, M. Canards in R^3 *J. Diff. Eq.*, **177** (2001)419–453

[14] M. Wechselberger Existence and Bifurcation of Canards in R^3 in the case of a Folded Node, preprint.